



Data Analysis Report

amPD-1 Effects in DIO and WT Mice - Serum

Client:

Author:

Date:

Contact: info@panomebio.com

Table of Contents

Experimental Methods	4
Sample preparation	4
Metabolomics assays	4
Data preprocessing	4
Statistical analysis	5
Results	6
Metabolite summary	6
Technical variation	8
Metabolite associations	9
Interpretation	13
Appendix	17

Project Summary

Sample description:

Forty mouse serum samples were received. Twenty of the samples were from DIO mice bearing MC-38 subcutaneous tumors and twenty of the samples were from WT mice with the same tumor model. Ten mice from both the DIO and WT groups were treated with amPD-1 the remaining ten in each group were untreated.

Goal:

To identify and characterize the metabolic differences between the serum of tumor-bearing DIO and WT and to determine the differential metabolic responses to amPD-1 treatment between WT and DIO mice.

Assay summary:

Global metabolomics assays were performed on all mouse samples, including polar and lipid fractions analyzed with both positive and negative ionization.

Analysis summary:

Global metabolomics data was processed with unbiased peak characterization and metabolite identification. Statistical analysis was performed to identify metabolites with significant alterations between the four sample groups. Amongst these metabolites, differences in response to amPD-1 treated was assessed.

Conclusions:

The results of the analysis show substantial metabolic alterations between tumor bearing DIO and WT mice. Of note, there were large differences between glycerophosphocholines and ceramide lipid species between DIO and WT mice. While the effects of amPD-1 treatment were smaller than the differences between DIO and WT mice, analysis revealed differential metabolic responses to amPD-1 treatment between DIO and WT mice. Overall, DIO mice were more metabolically sensitive to treatment than WT mice. The differentially affected metabolites indicated DIO-specific alternations in key metabolic pathways, including the pentose phosphate pathway.

Experimental Methods

Sample preparation

Sample handling and storage

Serum samples were frozen at -80°C after receipt. For analysis, samples were thawed on ice and vortexed prior to extraction.

Polar metabolite extraction

A $50\ \mu\text{L}$ aliquot of serum was transferred onto a solid phase extraction (SPE) system and $5\ \mu\text{L}$ was taken from each sample to form the pooled quality control sample. $200\ \mu\text{L}$ of 1:1 ACN:MeOH was added to each well and shaken for 1 min at room temperature at 360 rpm, followed by a 10 min incubation. Next, $150\ \mu\text{L}$ of 2:2:1 MeOH:ACN:H₂O was added to each well and taken again for 10 min. Polar metabolites were then eluted into the 96-well collection plate by using the positive pressure manifold. This is repeated with $100\ \mu\text{L}$ of 2:2:1 MeOH:CAN:H₂O into the same collection plate. Polar eluates were then covered and stored at -80°C until LC/MS analysis.

Lipid metabolite extraction

The SPE plates from the polar metabolite extraction were washed twice with 500 mL 1:1 MTBE:MeOH to elute lipids into a new collection plate. The combined eluates were dried under a stream of nitrogen at room temperature and reconstituted with $200\ \mu\text{L}$ 1:1 IPA:MeOH prior to LC/MS analysis.

Metabolomics assays

LC/MS analysis of polar metabolites

LC/MS mobile phases A and B were prepared as follows: A) 20mM ammonium bicarbonate, 0.1% ammonium hydroxide, 5% ACN, $2.5\ \mu\text{M}$ medronic acid and B) 95% ACN.

A 2 mL aliquot of polar metabolite extract was analyzed with HILIC/MS by using the following linear gradient at a flow rate of $250\ \mu\text{L}/\text{min}$: 0-1 min: 90% B, 1-12 min: 90-35% B, 12-12.5 min: 35-20% B, 12.5min-14.5 min: 20% B. The column was re-equilibrated with 20 column volumes of 90% B. Mass spectrometry analysis was completed with a mass range of 67-1500 Da with 1 scan/sec and a mass resolution of 120,000 in both positive and negative ionization mode.

LC/MS analysis of lipid metabolites

LC/MS mobile phases A and B were prepared as follows: A) 10 mM ammonium formate, 0.1% formic acid, $2.5\ \mu\text{M}$ medronic acid in 6:4 H₂O:ACN and B) 10 mM ammonium formate, 0.1% formic acid, $2.5\ \mu\text{M}$ medronic acid in 9:1 IPA:ACN.

A 2 mL aliquot of polar metabolite extract was analyzed with HILIC/MS by using the following linear gradient at a flow rate of $250\ \mu\text{L}/\text{min}$: 0-2 min: 30% B, 2-17 min: 30-75% B, 17-20 min: 75-85% B, 20-23 min: 85-100% B, 23-26 min: 100% B, 26-27 min: 100-30% B. The column was re-equilibrated for 5 min. Mass spectrometry analysis was completed with a mass range of 67-1500 Da with 1 scan/sec and a mass resolution of 120,000 in both positive and negative ionization mode.

Data preprocessing

Metabolite detection and identification

Metabolite signals (features) were detected in the LC/MS data through in-house peak detection and curation software. Features were aligned across samples and features with intensities greater than 1/3 of the corresponding intensity in the QC sample were classified as contaminants and removed from future analysis. Feature degeneracy (isotopes, adducts, fragments, etc.) were identified through clustering and ion assignment with in-house software.

Metabolites were structurally identified through searching against a database composed of known metabolites found in RefMet, LipidMaps, and HMDB and comparing isotope patterns and MS/MS fragmentation data (when available). Metabolite identifications were classified based on the Metabolomics Standards Initiative scoring scheme with values ranging from Level 2 to Level 4. Level 2 identifications were made on based on isotope pattern matches of greater than 90% similarity (reverse dot-product) and an MS/MS match of greater than 50% similarity (entropy similarity). Level 3 identifications were made based on an isotope pattern match with the same cutoffs as defined above. Level 4 identifications are signals determined to correspond to a unique metabolite that did not match to any compound in our metabolite database and are potentially novel compounds. For lipid compounds, the best matching lipid species is reported. However, the location of double bonds within acyl chains of a lipid species is not discernable from the LC/MS methods utilized. Thus, the double bond positions listed are not meaningful.

Data normalization and curation

Metabolomics data from all assays were concatenated. Metabolite signals were discarded if the coefficient of variation (CV) amongst the quality control samples was greater than 25%. Missing values were imputed by using half of the minimum detected intensity for each metabolite. Metabolite intensities were log₂ transformed prior to statistical analysis.

Metabolite identifications and intensities were manually reviewed for concordance and accuracy.

Statistical analysis

Hypothesis testing was performed with a two-tailed, one-way ANOVA with unequal variance across the four sample groups. Log₂ normalized metabolite intensities were used for null hypothesis testing. The resulting p-values were corrected with the Benjamini-Hochberg Procedure. Changes from amPD-1 treatment were assessed with a two-tailed t-test with unequal variance. Fold-changes were computed from non-log₂ intensities. Over-representation analysis was performed with a Fisher's Exact test comparing the expected number of metabolites found to be significant in each pathway with the number of significant metabolites found in each pathway. For null hypothesis testing, a corrected p-value cutoff of 0.05 and an absolute log₂ fold change of 1.0 was used. For the over-representation analysis, only the corrected p-value cutoff was used.

Results

Metabolite summary

Across the four assays used to profile the samples, 6,874 metabolites signals were detected and profiled (Figure 1). The relative abundance of each metabolite was quantified across each sample. Of the metabolites profiled, 257 could be identified with MSI Level 2 confidence (MS/MS and isotope pattern match) and 1,969 could be identified with MSI Level 3 (isotope pattern match) confidence. The metabolites identified in the polar fraction of the samples contained many organic acids, nucleic acids, and organic heterocyclic compounds. In the lipid data, a large number of glycerolipids and glycerophospholipids were also profiled (Figure 2).

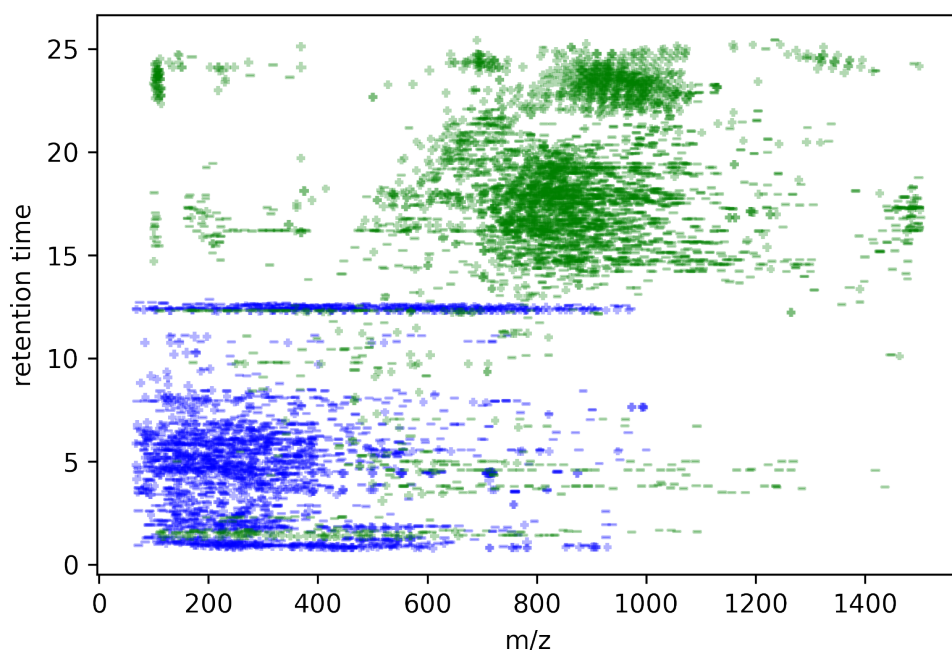


Figure 1: Detected metabolite signals. Each metabolite signal is represented by a point on the plot representing the m/z and retention time coordinates of the feature. Color of dots corresponds to the assay type (green = lipid, blue = polar) with the ionization mode indicated by the marker ("-" = negative mode, "+" = positive mode). The size of the points corresponds to the mean intensity of the signal.

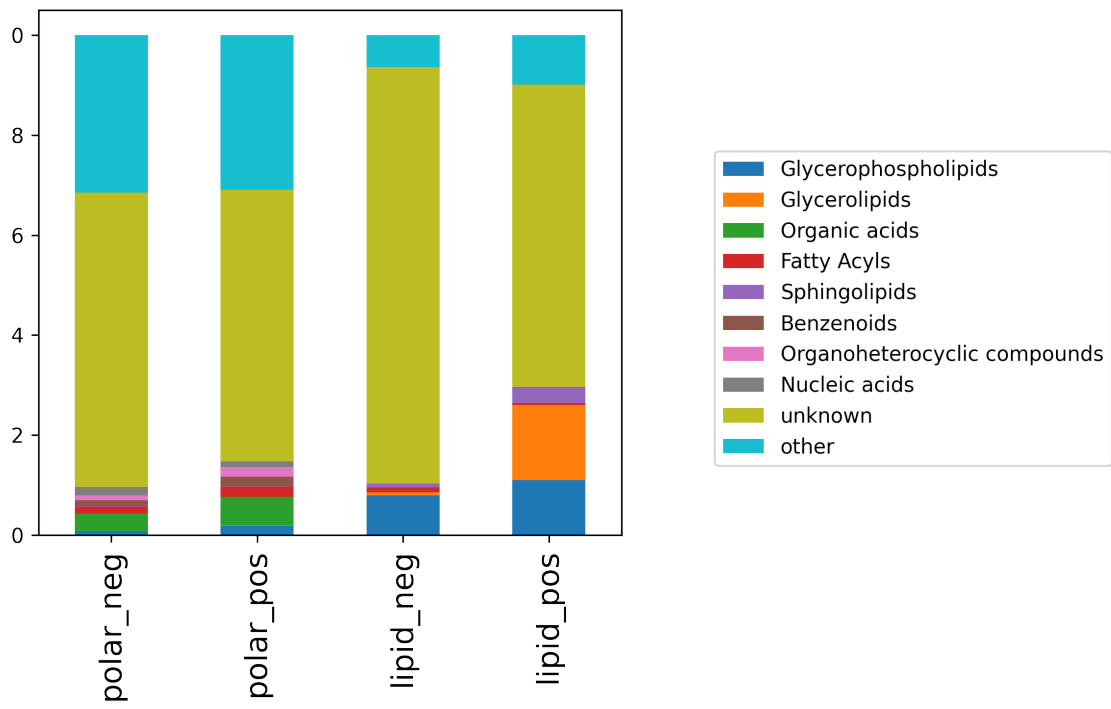


Figure 2: Chemical composition of identified metabolites. The chemical class composition is shown for each assay type. Unidentified metabolites are listed as unknown. Metabolites belonging to minor compound classes are listed as other.

Technical variation

A summary of the technical variation across the assays employed is shown below. Across all three assays, coefficient of variation (CV) values were generally less than 20% (Figure 3). Less than 1.0% of all measurements were missing values that required imputation.

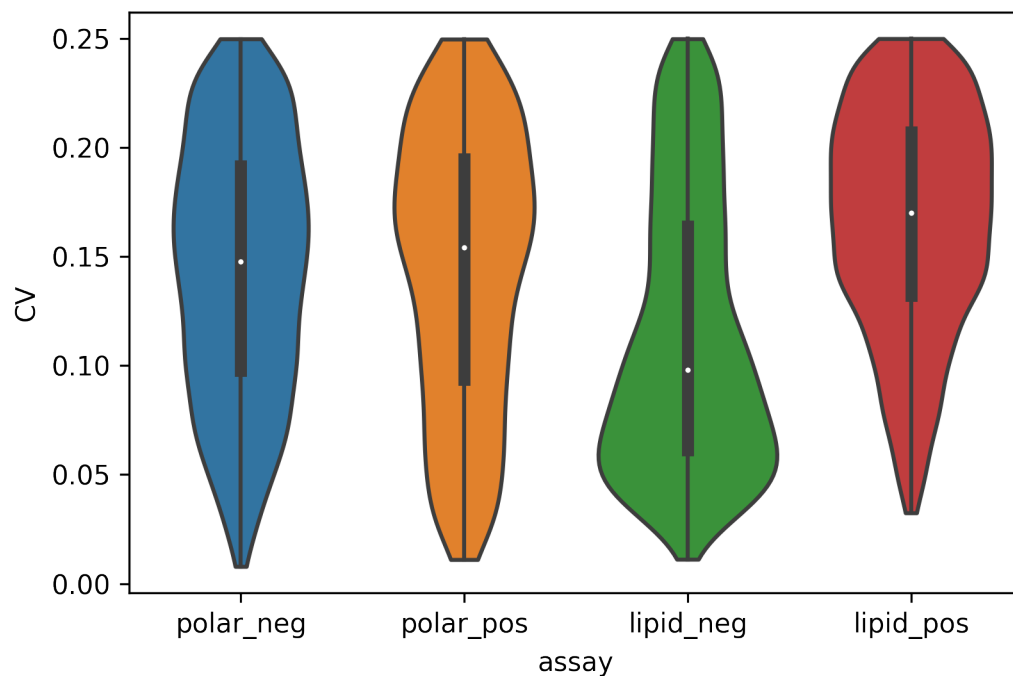


Figure 3: Coefficients of variation for profiled metabolites. The technical variation present in each assay is shown in the violin plot. The coefficient of variation (CV) is plotted from analysis of quality control samples.

Metabolite associations

The global trends in the metabolite profiles of samples are visualized below in the principal components analysis (Figure 4) and heatmap (Figure 5). Untreated WT samples are shown in blue, treated WT samples are shown in green, untreated DIO samples are shown in purple, and treated DIO samples are shown in red. As visible from these plots, there is clear clustering of samples into the WT and DIO groups. Minimal differences between treated and untreated samples are present in these unsupervised analyses.

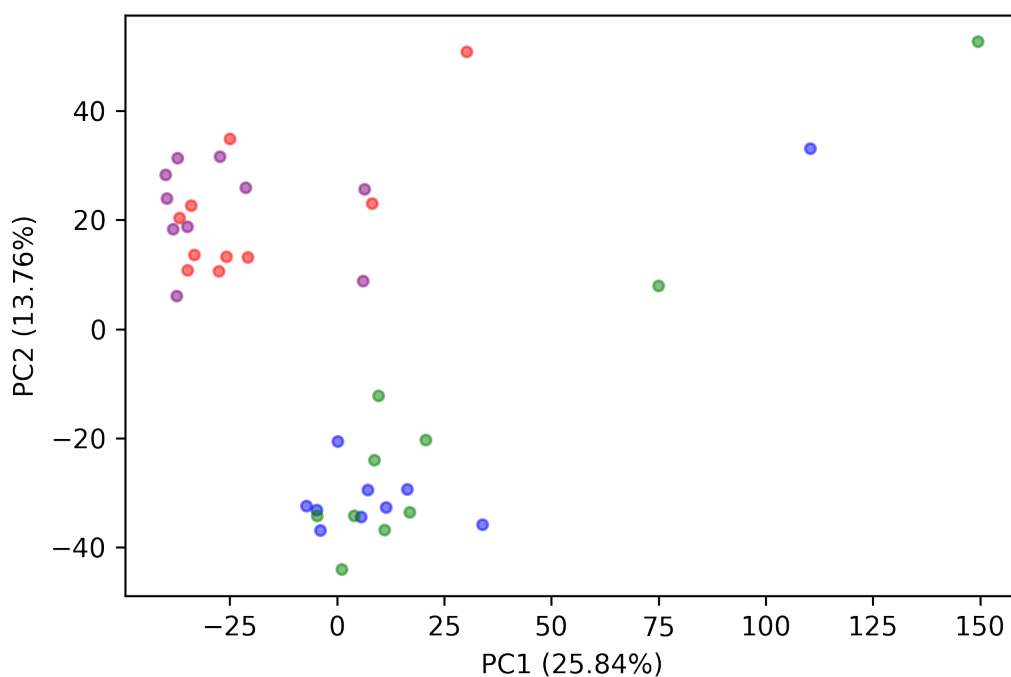


Figure 4: Principal components analysis of metabolomics data. The metabolic profiles (all assay results combined) for each sample are visualized in scatter plot above. Samples are colored according to experimental group.

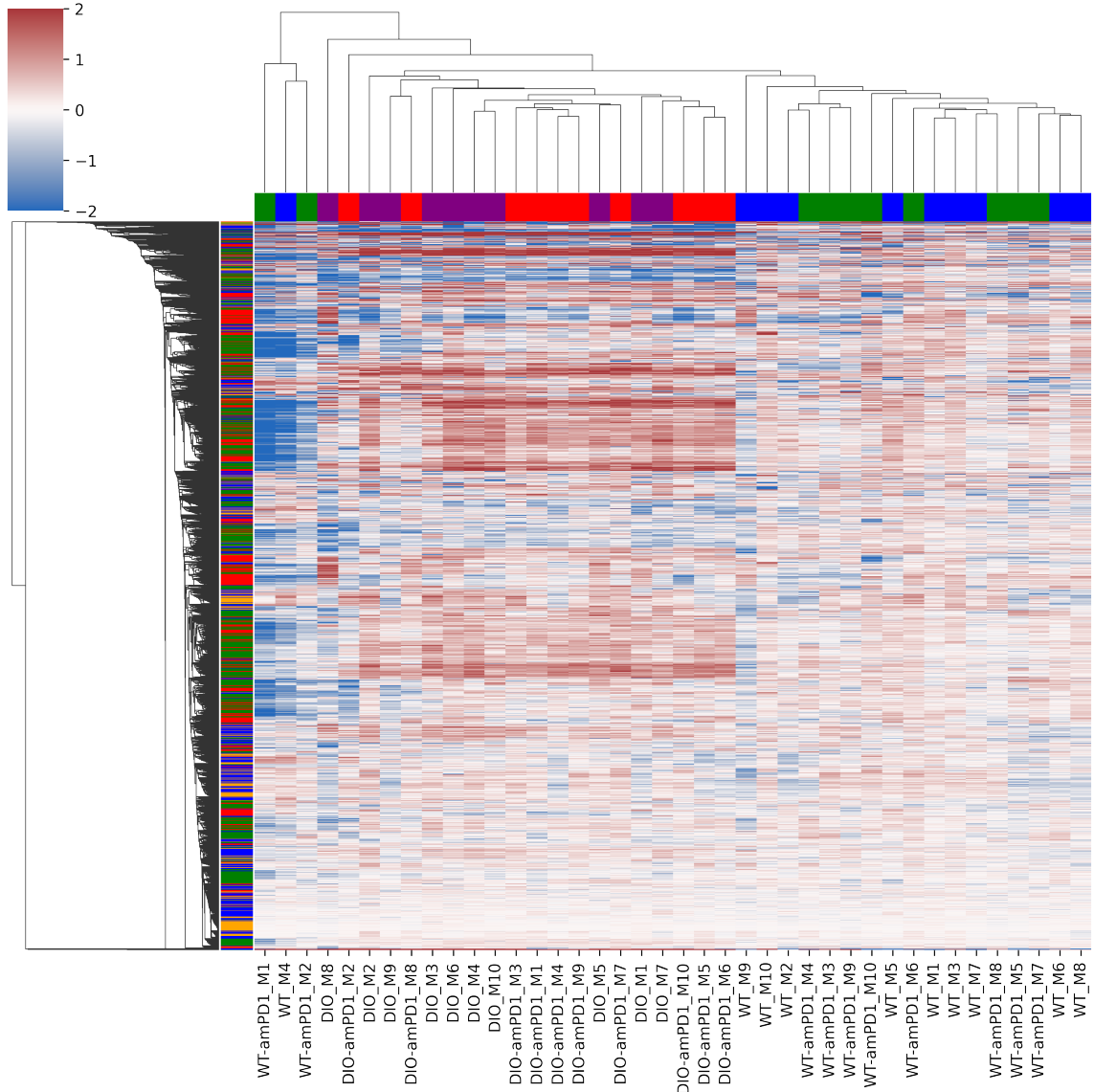


Figure 5: Heatmap of metabolomics data. The metabolic profiles (all assay results combined) for each sample are visualized in the heatmap above. Each column represents a sample, and each row represents a metabolite. Columns are colored according to experimental type. Rows are colored according to assay type (polar- = blue, polar+ = orange, lipid- = green, lipid+ = red). The color of each cell indicates the $\log_2(\text{fc})$ relative to the mean WT level of each metabolite.

To determine specific metabolic alternations between the four sample groups, null hypothesis testing was performed on all profiled metabolites, revealing 1,536 significantly altered metabolites (having a corrected p-value (q) of less than 0.05) between at least two of the sample groups. The top fifty most significant metabolites are shown in Figure 6. The largest alterations are between DIO and WT samples with many metabolites having increased or decreased circulating concentrations.

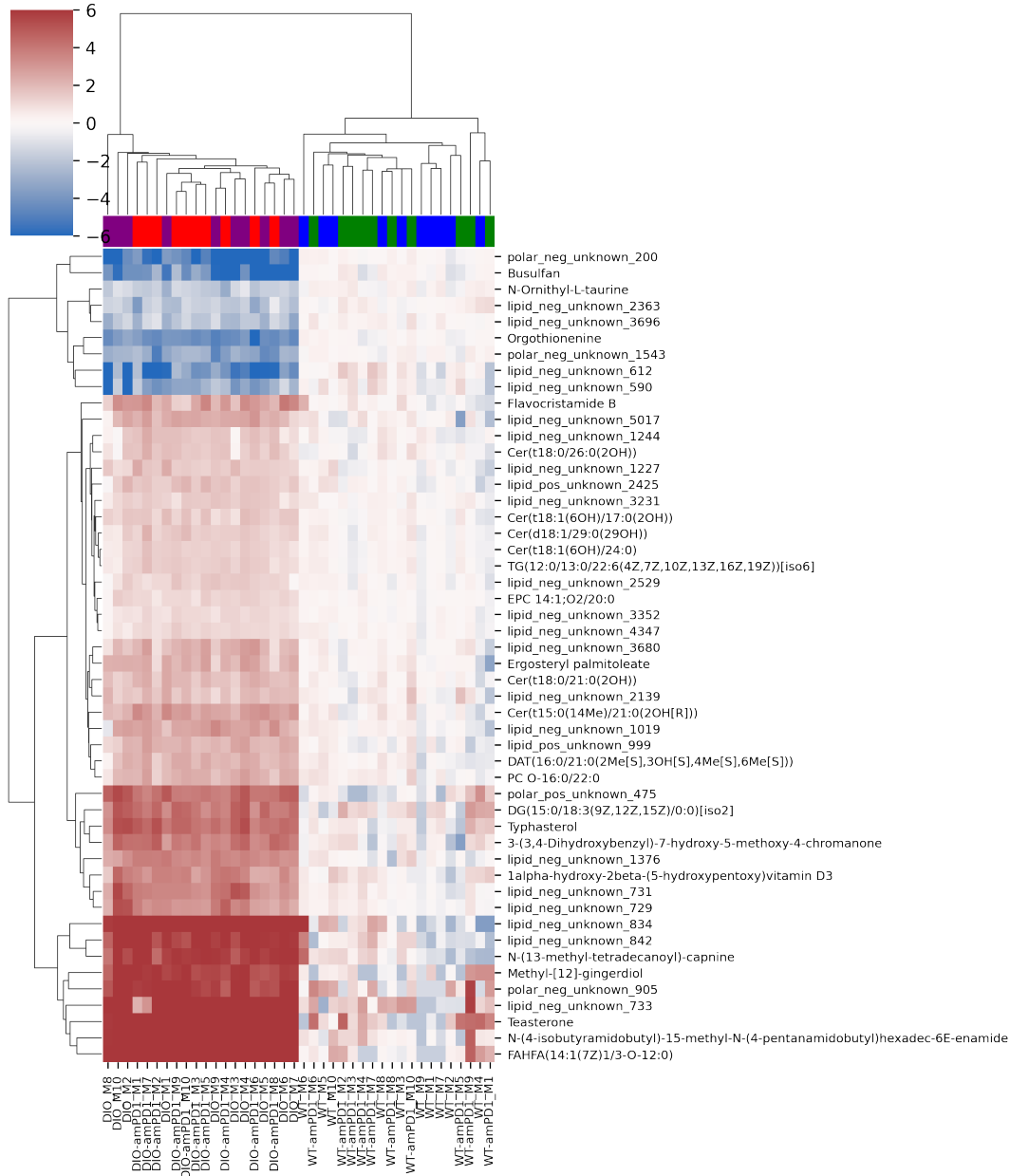


Figure 6: Heatmap of significantly altered metabolites. The log₂ fold-changes of the top 50 most significantly altered metabolites are plotted for each experimental group.

To determine specific metabolic alternations coming from amPD-1 treatment, null hypothesis testing between both treated and untreated WT and DIO samples was performed on the 1,536 metabolites elucidated in the previous analysis. In total, 213 of these compounds had a statistically significant difference (p -value < 0.05) between treated and untreated samples in at least one sample group (DIO or WT mice). The fold-changes relative to the untreated groups of DIO and WT mice are shown below in Figure 7. The DIO mice showed an overall stronger response to amPD-1 treatment with the majority of these metabolites only showing a response in DIO mice (Figure 8).

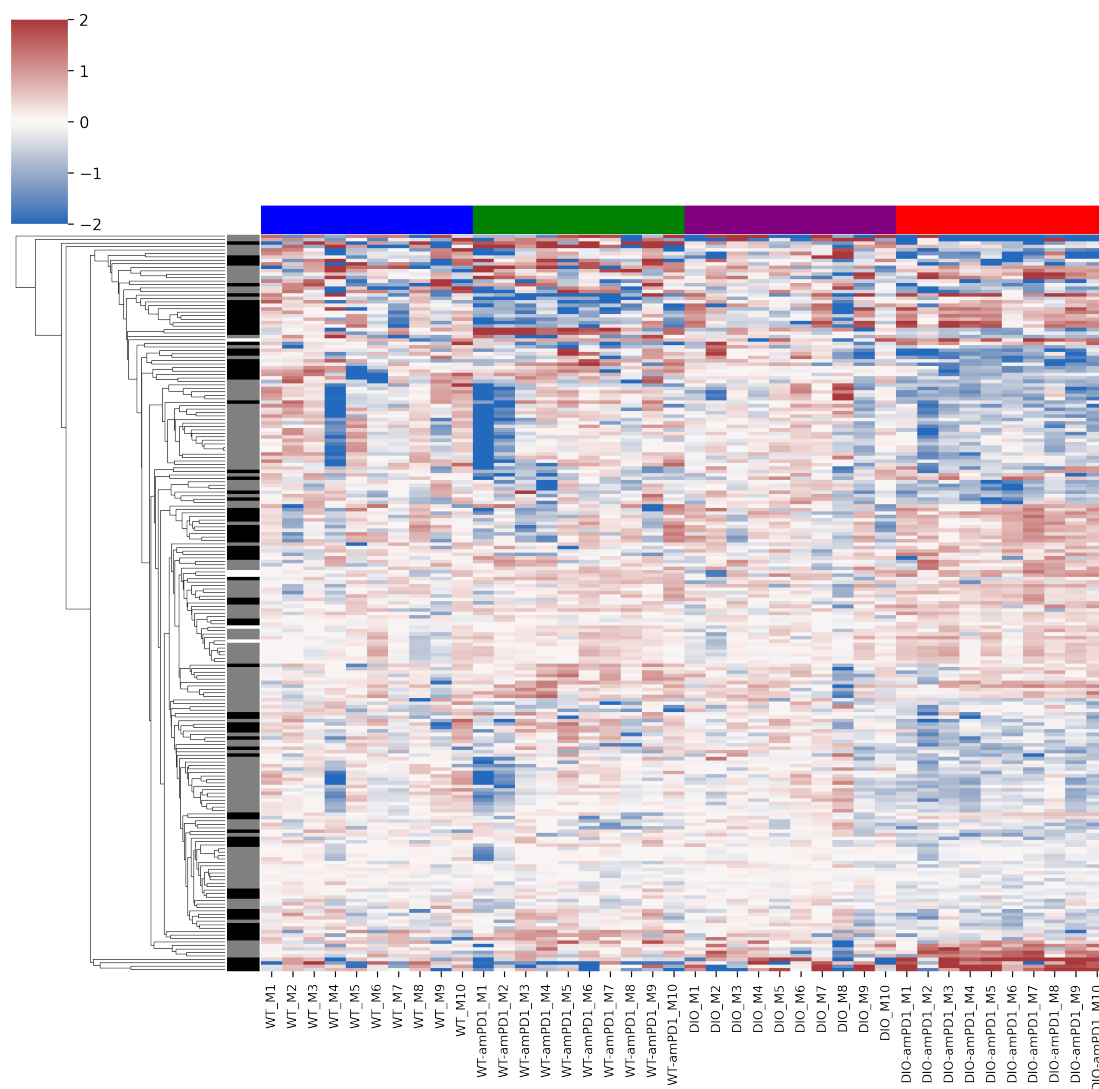


Figure 7: Heatmap of metabolites altered with amPD-1 treatment. The log₂ fold-changes (relative to the mean abundance in the untreated samples of each group) of the metabolites significantly altered (p -value < 0.05) between DIO treated vs. untreated or WT treated vs. untreated are plotted for each experimental group. Columns are colored according to experimental group. Rows are colored as follows: black) an opposite fold-change signature between DIO and WT samples, grey) direction of change in the same between DIO and WT samples but the alteration is only significant in one of the sample types, white) the direction of change is the same and the effects are significant in both WT and DIO mice.

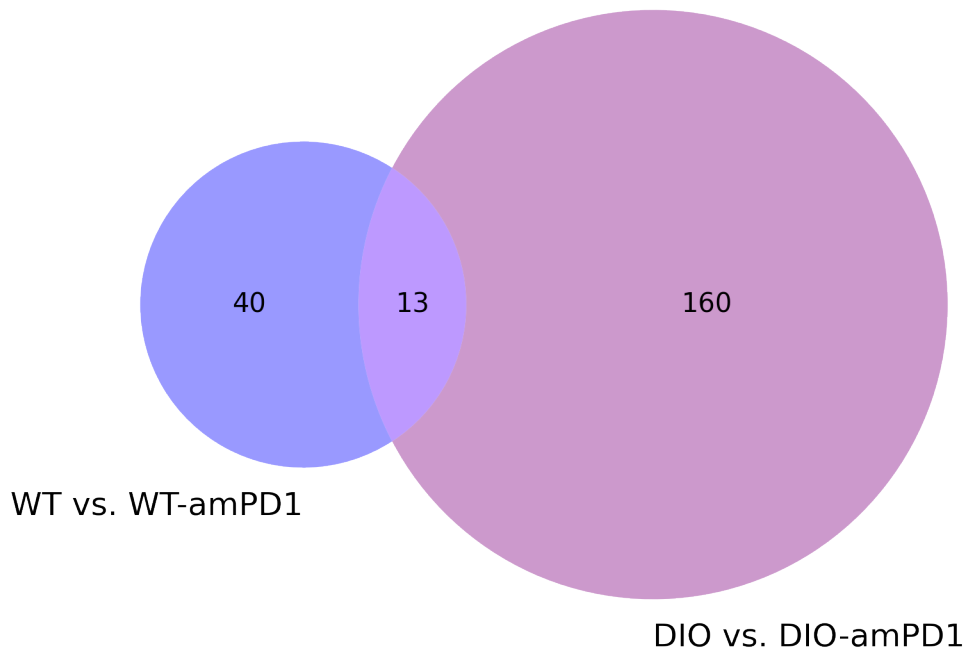


Figure 8: Venn diagram of treatment effects in DIO and WT mice. The significant metabolite alterations between treated and untreated DIO and WT mice are compared in the Venn diagram above. The WT and DIO mice show little similarity in the metabolic signature of treatment.

Strikingly, 78 of the metabolites with a treatment effect in DIO or WT mice show a different direction of change in DIO and WT mice (e.g., increased metabolite level after treatment in DIO mice but decreased after treatment in WT mice). These metabolites are shown in Figure 9.

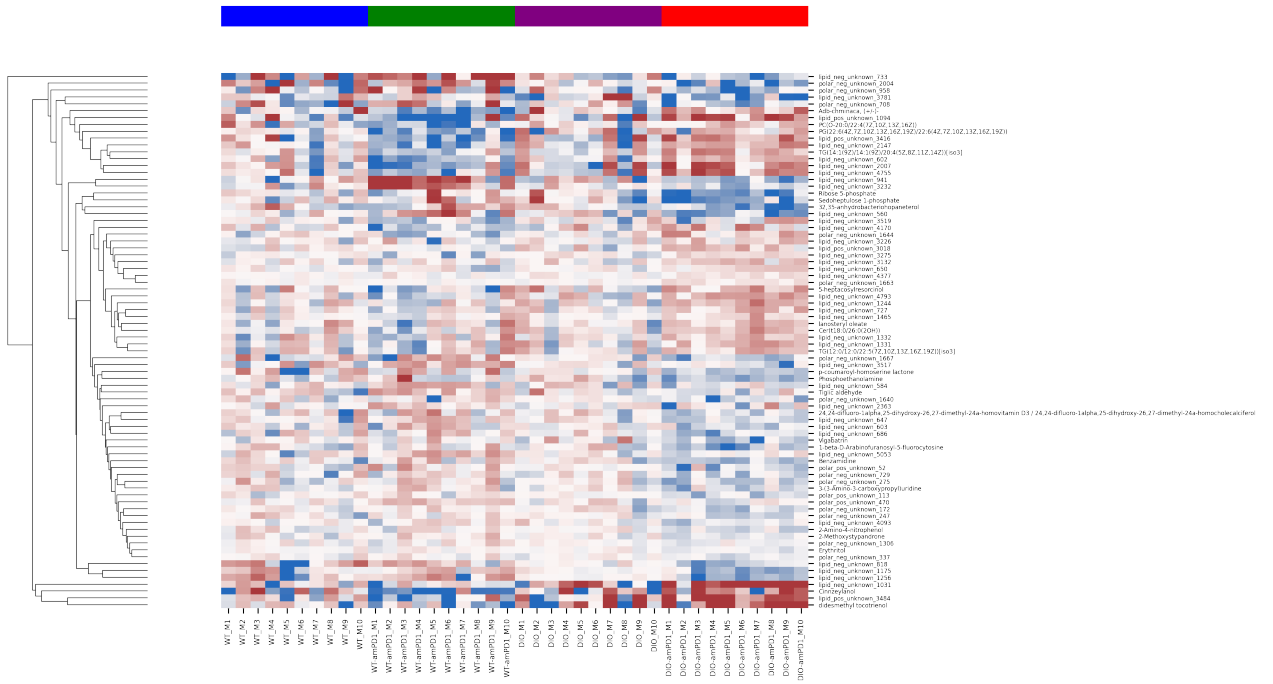
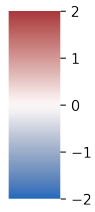


Figure 9: Heatmap of metabolites differentially altered with amPD-1 treatment. The log₂ fold-changes (relative to the mean abundance in the untreated samples of each group) of the metabolites significantly altered (p-value < 0.05) between DIO treated vs. untreated or WT treated vs. untreated but in different directions are plotted for each experimental group. Columns are colored according to experimental group.

Interpretation

To gain biological insight into the metabolite alterations detected across all four sample groups, an over-representation analysis was performed which identified key lipid classes altered between DIO treated, DIO untreated, WT treated, and WT untreated samples (Figure 10). These results were driven by the broad alterations between DIO and WT samples that occur independent of the treatment effect. The analysis revealed multiple lipid classes were over represented with ceramides being the most over-represented groups. Of the thirty-two ceramides profiled in this experiment, twenty-three showed a significant difference between at least two of the sample groups.

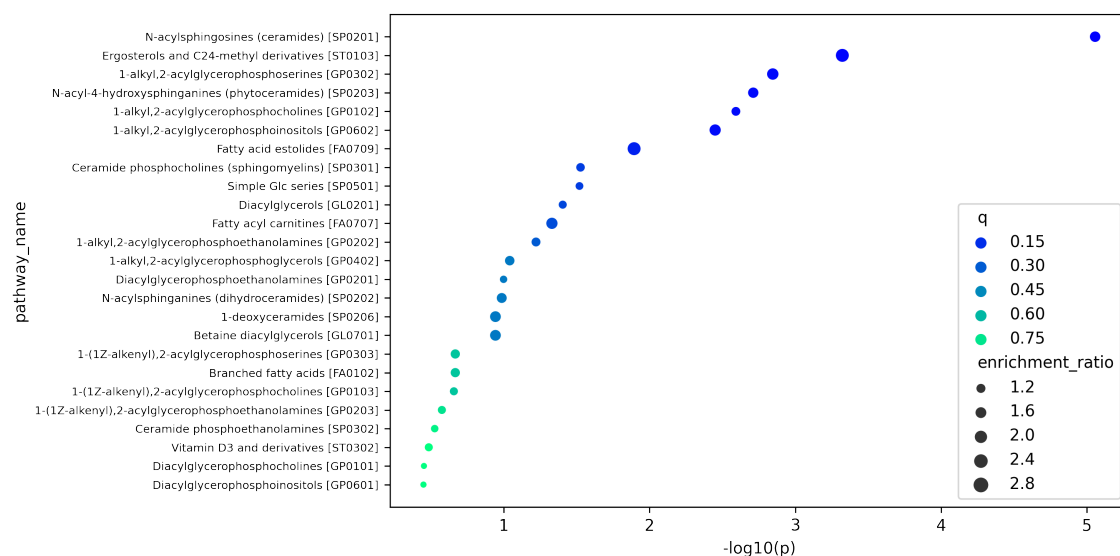


Figure 10: Pathway analysis of significant metabolites. The pathways found to be enriched are shown with their corresponding significance levels.

In addition to the overall differences between WT and DIO mice, the results of the analyses performed clearly show differences in the treatment effect of amPD-1 between WT and DIO mice. In particular, DIO mice show a much higher level of metabolic alteration as a result of drug treatment. In examining the metabolites that show opposite effects as a result of amPD-1 treatment, we see many polar and lipid metabolites changes coming from both unknown and identified compounds. Of particular note is pentose phosphate pathway intermediates: ribose 5-phosphate (Figure 11) and sedohepulose 1-phosphate (Figure 12). These metabolites show a strong effect only in DIO treated. Given the reliance on nucleotide synthesis (which relies on the pentose phosphate pathway) for proliferation of cancer cells, these findings may warrant further investigation into amPD-1 interaction with the pentose phosphate pathway.

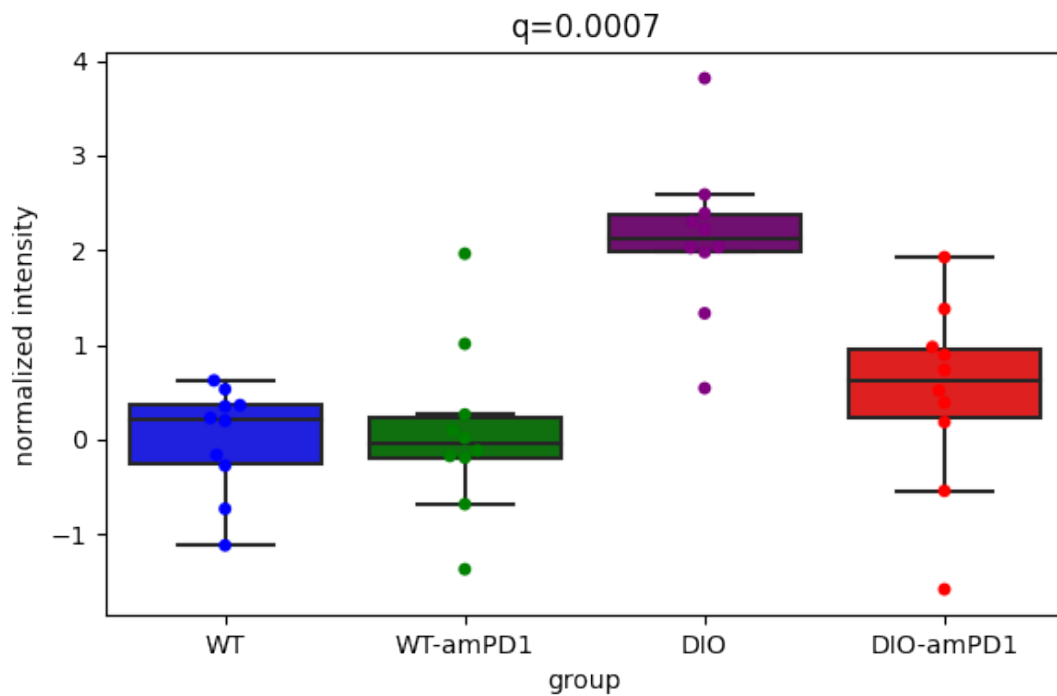


Figure 11: Ribose 5-phosphate levels in each group. The normalized abundance of ribose 5-phosphate is shown for each group and sample.

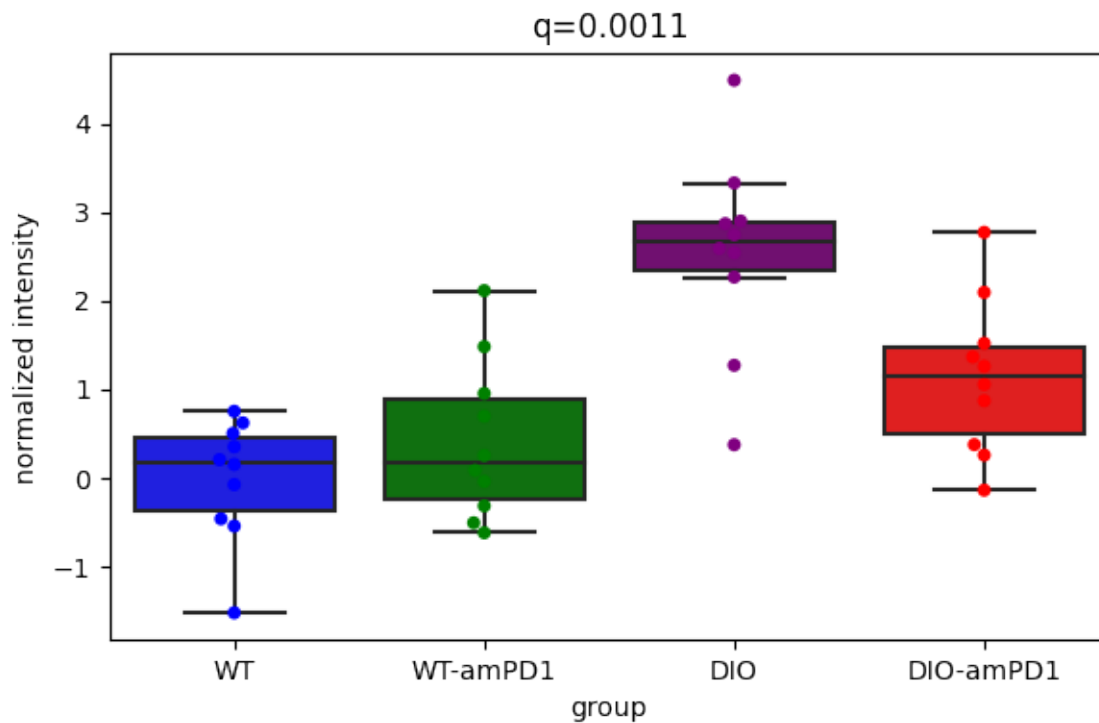


Figure 12: Sedoheptulose 1-phosphate levels in each group. The normalized abundance of sedoheptulose 1-phosphate is shown for each group and sample.

Many other metabolites showed DIO-specific responses including key lipid metabolites, such as phosphoethanolamine (a precursor for phospholipids). In addition, the large number of unknown compounds that show this DIO-specific response presents an exciting opportunity to elucidate potentially novel metabolites that mediate the effects of amPD-1. In general, however, metabolite alterations detected from drug treatment had relatively small effect sizes. While the broad differences between DIO and WT mice were able to be well characterized with the sample numbers in this study, replication with increased sample numbers is recommended to confirm the amPD-1 alterations reported.

Appendix

Supplementary Files

1. SupplementaryTables.xlsx: excel file containing sample metadata, technical variation metrics for each metabolite, all detected unique metabolite features and their raw intensities and normalized intensities, the metabolite identifications and confidence for each feature, the detailed results of the statistical analyses.
2. raw_data.zip: raw data in an open (.mzML) format.
3. Plots.zip: high-resolution images for all figures in this report as well as boxplots showing the intensity of each metabolite across all experimental conditions.

Glossary

1. LC/MS: Liquid chromatography couple to mass spectrometry. The analytical technique used for the metabolite assays.
2. Retention time: The elution time of metabolites in the LC portion of the analysis. Retention time is determined by the chemical properties of the metabolite (e.g., hydrophobicity)
3. m/z: The mass (m) to charge (z) ratio of the measured ions in the MS portion of the analysis. In metabolomics, the charge of the metabolites is typically one or two. Thus, this can be thought of as just the molecular mass of the ions.
4. Features/metabolites signals: Signals in the raw data that represent unique compounds or metabolites measured in the LC/MS experiment.
5. Intensity: The relative abundance of the compound/metabolite in the sample.
6. Quality control sample: A sample repeatedly analyzed to measure system stability and determine signal drift.



**Contact us to
initiate a project**

www.panomebio.com

info@panomebio.com

4340 Duncan Avenue, St. Louis, MO